J. Marine. Sci. Appl. (2013) 12: 381-392
DOI: 10.1007/s11804-013-1208-8

Interaction of Water Waves with Small Undulations on a Porous Bed in a Two-layer Ice-covered Fluid

Srikumar Panda and S. C. Martha*

Department of Mathematics, Indian Institute of Technology Ropar, Rupnagar 140001, Punjab, India

Abstract: The scattering problem involving water waves by small undulation on the porous ocean-bed in a two-layer fluid, is investigated within the framework of the two-dimensional linear water wave theory where the upper layer is covered by a thin uniform sheet of ice modeled as a thin elastic plate. In such a two-layer fluid there exist waves with two different modes, one with a lower wave number propagate along the ice-cover whilst those with a higher wave number propagate along the interface. An incident wave of a particular wave number gets reflected and transmitted over the bottom undulation into waves of both modes. Perturbation analysis in conjunction with the Fourier transform technique is used to derive the first-order corrections of reflection and transmission coefficients for both the modes due to incident waves of two different modes. One special type of bottom topography is considered as an example to evaluate the related coefficients in detail. These coefficients are depicted in graphical forms to demonstrate the transformation of wave energy between the two modes and also to illustrate the effects of the ice sheet and the porosity of the undulating bed.
Keywords: two-layer fluid; wave scattering; reflection and transmission coefficients; linear water wave theory; Fourier transform; perturbation technique; small undulation; porous bed

Article ID: 1671-9433(2013)04-0381-12

1 Introduction

Understanding the problems involved with wave propagation over an obstacle in a two-layer fluid and developing solutions to these problems is important for their possible applications in costal hydrodynamics, and as a result these problems have been studied by scientists and engineers for the last few decades. For two-layers of incompressible and inviscid fluid, separated by a common interface, with the upper layer fluid of lower density having a free surface, Lamb (1932) has shown that for a given frequency, time-harmonic small amplitude gravity waves with a lower wave number (mode) propagate along the free surface while those with a higher wave number propagate along the interface. When a train of progressive waves of a particular mode encounter an obstacle, the wave train is partially reflected into waves of both modes and are also partially transmitted into both modes. Thus there is a transfer of energy from the surface wave to the interface wave and vice versa.

Linton and McIver (1995) considered the problem based on the linear wave theory concerning the interaction of water waves with horizontal cylinders in a fluid consisting of a layer of finite depth bounded above by a free surface and below by an infinite layer of fluid of greater density. They obtained the reflection and transmission coefficients for different wave numbers due to the incident wave of different wave numbers. Linton and Cadby (2002) extended the problem of Linton and McIver (1995) to oblique water wave scattering and solved this particular problem by using multipole expansion. Later on, Chamberlain and Porter (2005) studied the problem involving the scattering of water waves in a two-layer fluid of varying mean depth in a three-dimensional context using linear theory. They used variational techniques to construct a particular type of approximation that had the effects of removing the vertical coordinate and reducing the problem to two coupled partial differential equations in two independent variables.

Christodoulides and Dias (1995) examined the problem involving periodic capillary-gravity waves at the interface between two bounded fluids of different density using weakly nonlinear analysis. A relation between wave frequency and wave amplitude was obtained. They also discussed about the stability of travelling and standing waves with respect to three-dimensional modulation. Based on the quantum mechanical scattering theory, Olbers (1981) analyzed the scattering of internal waves when localized in homogeneities, like topographic features, variations of the mean sea level, and jet-like currents, in the oceanic waveguide. Sveen *et al*. (2002) examined a series of quantitative laboratory studies to determine the spatial and temporal development of the velocity, vorticity and density field associated with the flow of an internal solitary wave. Bhatta and Debnath (2006) analyzed transient two layer fluid flows over a viscoelastic ocean bed and solved the problem using the Laplace transform and the Fourier transform.

When the obstacle appears in the form of small undulations at the bottom, the problem involving reflection of water waves by patches of bottom undulation has received an increasing amount of attention as its mechanism is important in the development of shore parallel bars. Davies (1982)

Received date: 2013-05-15.
Accepted date: 2013-06-19.
Foundation item: Supprted by the ISIRD grant (Ref. No. 16-3/10/IITRPR/Acad/116).
***Corresponding author Email:** scmartha@iitrpr.ac.in

considered the problem involving reflection of normally incident surface waves by a patch of sinusoidal bottom undulation for a single layer fluid and solved the problem using the Fourier transform technique. Martha and Bora (2007) solved the problem involving oblique scattering of surface waves by a small undulation on the bottom of a single layer fluid by using the Finite cosine transform technique.

Mohapatra and Bora (2009) considered the problem involving scattering of internal waves in a two-layer fluid over a channel. Based on perturbation and Green's function technique they derived the reflection and transmission coefficients up to the first order in terms of integrals involving the shape function representing the bottom undulation. Maiti *et al*. (2009) analyzed the diffraction of interface waves in two layer fluid by using Green's function technique and obtained the quantities of physical interest, namely the reflection and transmission coefficients. Mohapatra and Bora (2012) extended their problem for oblique wave scattering and successfully obtained the solution with the help of Green's function technique.

The above works are related to the water wave problems without giving consideration to the ice-cover at the surface. In recent times, due to the increase in scientific activities in the Polar Regions, many researchers have shown an interest in the investigation of ice-wave interaction problems. For example, Fox and Squire (1994), Chakrabarti (2000), Tkacheva (2001), Chung and Fox (2002) and others have analyzed various types of water wave problems in an ice-covered ocean where the ice cover is modelled as a thin elastic plate. The researchers are interested in studying these interaction problems due to their possible applications in the areas of coastal and marine engineering and other practical areas. One practical example is to understand the effects of wave propagation through the marginal ice zones in Antarctica. These kinds of problems are also considered for modelling floating breakwaters and very large floating structures like off-shore pleasure resorts, floating airports, floating oil storage bases etc.

All the above works were focused only on the solutions of the water wave interaction problems where the ocean bed is not permeable. If the bottom is composed of some specific type of porous materials, non-rigid, the effects of porosity on the hydrodynamic coefficients will be an important aspect of the study. In practical terms, the flow of fluid into the porous media leads to different phenomena like wave energy dissipation, damping etc. as reported in the literatures. Water wave interaction with the porous media was studied by many scientists like Chakrabarti (1989), Jeng (2001) and references therein. Mase and Takeba (1994) focused on the Bragg scattering of gravity waves over a permeable sea bed. Zhu (2001) considered the problems involving wave propagation within porous media on an undulating bed in a single layer and developed a solution by employing the Galerkin eigenfunction expansion technique. They investigated the wave reflection coefficient numerically. Gu and Wang (1991) investigated the interaction of water waves with a rigid porous seabed in a single layer both theoretically and experimentally. Silva *et al*. (2002) discussed the water wave reflection and transmission problem in a single layer where a porous medium was assumed to lie on an ocean-bed of varying quiescent depths. Martha *et al*. (2007) considered the problem of water wave scattering by small undulation on a porous bed in a single layer.

In the present study, we consider surface wave scattering by small undulation on a porous ocean-bed in a two-layer fluid whose upper layer is covered by a very thin uniform ice-sheet modeled as a thin elastic plate. In this case, time-harmonic progressive waves of a particular frequency can propagate with two different wave numbers: waves with a lower wave number propagate at the ice-cover and the other with a higher wave number propagates at the interface. The motion of the fluid inside the porous bed is not analyzed here and it is assumed that the fluid motions are such that the bottom condition as is used here holds good and depends on a known parameter G, called the porosity parameter as reported in the notes by Martha *et al*. (2007). By employing Perturbation analysis involving a small parameter $\varepsilon(\ll 1)$ being present in the representation of the small undulations of the porous ocean-bed, the governing BVPs are reduced to simpler BVPs. The solution of the zeroth order BVP is obvious. The BVPs at the first order are solved by using the Fourier transform technique to obtain the first-order velocity potentials and these potentials are utilized in obtaining the first-order reflection and transmission coefficients in terms of integrals involving the shape function $c(x)$ representing the bottom undulation. From the application point of view, a patch of sinusoidal ripples is taken as an example to evaluate the integrals for reflection and transmission coefficients. The numerical values for the first order reflection and transmission coefficients of various modes due to normal incident waves of two different modes are computed and depicted graphically to demonstrate the transformation of wave energy between two modes in the presence of porosity at the bed.

2 Mathematical formulations

The geometry of the two-layer fluid is shown in Fig. 1. Here, the upper layer is of finite depth h and is covered by a thin uniform ice sheet of infinite length, while the bottom layer has small undulations. Each fluid is ideal, inviscid, incompressible, and immiscible having constant but different densities. The effects of surface tension at the surface of separation is neglected. We use the right hand side Cartesian coordinate system with the (x,y)-plane lying in the mean position of the interface and the y-axis is measured vertically downward from the undisturbed interface between the two fluids. The porous bed, the bottom of the lower layer having small undulation is described by $y = H + \varepsilon c(x)$. Here, $c(x)$ is a bounded and continuous function, describing the shape of the undulation and $c(x) \to 0$ as $|x| \to \infty$ so that the ocean is of uniform finite depth H far away from the undulation on either side, $\varepsilon(\ll 1)$ is a small parameter giving a measure of the smallness of the undulation. In this article, the ice sheet is modelled as a thin elastic plate and the motion of the fluid inside the porous bed is not analyzed. The upper layer $-h \le y \le 0$, is referred to as region I, whilst the lower layer $0 \le y \le H + \varepsilon c(x)$ is referred to as region II. The velocity potential in the upper layer is ψ and in the lower layer is ϕ.

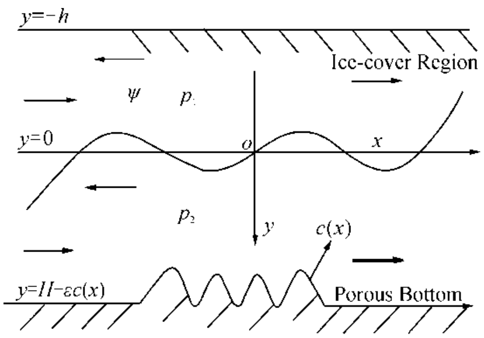

Fig. 1 Definition sketch

The motion is assumed to be irrotational and so both ψ and ϕ satisfy Laplace's equations:

$$\frac{\partial^2\psi}{\partial x^2}+\frac{\partial^2\psi}{\partial y^2}=0 \qquad \text{in region I} \tag{1}$$

$$\frac{\partial^2\phi}{\partial x^2}+\frac{\partial^2\phi}{\partial y^2}=0 \qquad \text{in region II} \tag{2}$$

Assuming the density of the fluid in the upper layer is ρ_1 and in the lower layer ρ_2 with $\rho_1 < \rho_2$, the linearized boundary conditions on the upper surface, interface and bottom are:

$$K\psi + \left(1-\delta K + D\frac{\partial^4}{\partial x^4}\right)\psi_y = 0, \text{ on } y=-h, \tag{3}$$

$$\psi_y = \phi_y, \quad \text{on } y=0, \tag{4}$$

$$\rho\left(K\psi+\psi_y\right) = K\phi + \phi_y, \quad \text{on } y=0, \tag{5}$$

$$\frac{\partial\phi}{\partial n} - G\phi = 0 \qquad \text{on } y = H+\varepsilon c(x) \tag{6}$$

where $\rho = \rho_1/\rho_2\,(<1)$, $K=\sigma^2/g$, the time-dependence of $e^{-i\sigma t}$ having been suppressed, g is the acceleration due to gravity, G is the porous effect parameter corresponding to the ocean-bed, $\partial/\partial n$ denotes the normal derivative at a point (x,y) on the bottom, δ is a constant having the dimension of the length and D is given by:

$$D = \frac{Eh_0^3}{12\left(1-\upsilon^2\right)\rho_1 g}$$

with E being Young's modulus, υ being Poisson's ratio and h_0 is the very small thickness of the ice-sheet.

The boundary conditions (3), (4) and (5) represent the linearized ice-cover condition, the continuity of normal velocity and pressure at the interface, respectively. Now the equation (6) can be approximated as:

$$\frac{\partial\phi}{\partial y} - \varepsilon\frac{\partial}{\partial x}\left[c(x)\frac{\partial\phi}{\partial x}\right] - G\left[\phi + \varepsilon c(x)\frac{\partial\phi}{\partial y}\right] + O\left(\varepsilon^2\right) = 0 \qquad y=H \tag{7}$$

Within this framework in the two-layer fluid system, a train of time-harmonic progressive waves takes the form:

$$\psi(x,y) = f(u,y)e^{\pm iux} \qquad \text{in } -h \le y \le 0 \tag{8}$$

$$\phi(x,y) = \left[\cosh u(H-y) - \frac{G}{u}\sinh u(H-y)\right]e^{\pm iux} \qquad \text{in } 0 \le y \le H \tag{9}$$

where,

$$f(u,y) = \frac{\left[\sinh uH - \frac{G}{u}\sinh uH\right]\left(\left(Du^4+1-\delta K\right)u\cosh u(h+y) - K\sinh u(h+y)\right)}{K\cosh uh - \left(Du^4+1-\delta K\right)u\sinh uh} \tag{10}$$

with u satisfying the dispersion relation

$$\begin{aligned}\Delta(u) \equiv{}& u^2(1-\rho)\left(Du^4+1-\delta K\right) - \\ & Ku\left[\left(Du^4+1-\delta K\right)\left(\rho\coth uh + \coth uH\right) + (1-\rho)\coth uh\right] + \\ & K^2\left(\rho + \coth uh\coth uH\right) + \\ & GK\left[2+\left(Du^4-\delta K\right)(1+\rho)\right]\coth uh\coth uH - \\ & \left(Du^4+1-\delta K\right)uG(1-\rho)\coth uH - \\ & \frac{K^2G}{u}\left(\coth uh + \rho\coth uH\right) = 0\end{aligned} \tag{11}$$

The dispersion relationship (11) has two positive real roots m and M which indicate the propagating modes; a complex conjugate pair of roots corresponding to the damped propagating modes and a countable infinity purely imaginary roots corresponding to a set of evanescent modes. Due to the evanescent mode of waves appearing in a fluid region, when the incident wave is scattered, a part of the incident interfacial wave may become trapped and may lead to a standing wave pattern over the bottom irregularities. This phenomenon is called the *Anderson localization*. Since these waves do not affect the asymptotic behavior of the resultant reflected and transmitted waves, any type of localization is not considered while formulating and solving the present problem. More information related to the Anderson localization can be found in Guazzelli *et al*. (1983), Devillard *et al*. (1988) and Ye (2004).

Since the dispersion relation has only two positive real roots m and M, say ($m<M$), there exists two modes of propagating waves. The wave of mode m propagates at the ice-cover while the wave of mode M propagates at the

interface.

Now we consider a normal incident progressive wave of mode m, in the form:

$$\psi_0(x,y) = f(m,y)\mathrm{e}^{\mathrm{i}mx} \text{ in } -h \le y \le 0, \tag{12}$$

$$\phi_0(x,y) = \left[\cosh m(H-y) - \frac{G}{m}\sinh m(H-y)\right]\mathrm{e}^{\mathrm{i}mx} \text{ in } 0 \le y \le H \tag{13}$$

When there is a normal incident of the progressive wave from the direction $x=-\infty$ on the bottom undulation then the far-field behaviors of ψ and ϕ, respectively, are given by:

$$\psi(x,y) \to \begin{cases} f(m,y)\left(\mathrm{e}^{\mathrm{i}mx} + r^m \mathrm{e}^{-\mathrm{i}mx}\right) \\ \quad + R^m f(M,y)\mathrm{e}^{-\mathrm{i}Mx} \quad \text{as } x \to -\infty, \\ t^m f(m,y)\mathrm{e}^{\mathrm{i}mx} \\ \quad + T^m f(M,y)\mathrm{e}^{\mathrm{i}Mx} \quad \text{as } x \to \infty, \end{cases} \tag{14}$$

and

$$\phi(x,y) \to \begin{cases} \begin{bmatrix} \cosh m(H-y) \\ -\dfrac{G}{m}\sinh m(H-y) \end{bmatrix}\left(\mathrm{e}^{\mathrm{i}mx} + r^m \mathrm{e}^{-\mathrm{i}mx}\right) + \\ \quad R^m \begin{bmatrix} \cosh M(H-y) \\ -\dfrac{G}{M}\sinh M(H-y) \end{bmatrix}\mathrm{e}^{-\mathrm{i}Mx} \quad \text{as } x \to -\infty \\ t^m \begin{bmatrix} \cosh m(H-y) \\ -\dfrac{G}{m}\sinh m(H-y) \end{bmatrix}\mathrm{e}^{\mathrm{i}mx} + \\ \quad T^m \begin{bmatrix} \cosh M(H-y) \\ -\dfrac{G}{M}\sinh M(H-y) \end{bmatrix}\mathrm{e}^{\mathrm{i}Mx} \quad \text{as } x \to \infty, \end{cases} \tag{15}$$

where the unknown coefficients r^m, R^m in relations (14) and (15) are respectively the reflection coefficients associated with reflected waves of modes m and M, due to a normal incident wave of mode m. Similarly in relations (14) and (15), the unknowns t^m and T^m denote the transmission coefficients associated with transmitted waves of modes m and M respectively, due to a normal incident wave of mode m. These unknown coefficients are to be determined here.

Similarly, when we consider the incidence of progressive waves of mode M, we will have two other far-field conditions with another four unknown coefficients (reflection and transmission) which are also to be determined.

3 Method of solution

3.1 Perturbation analysis

Let us first consider a train of progressive waves of mode m to have normal incidents on the bottom undulation. If there is no undulation at the bottom, the interface wave train will propagate without any obstruction and there will be transmission only. In view of this along with the approximate form of relation (7), ψ, ϕ, t^m, r^m, T^m and R^m can be expressed in terms of the small parameter ε as follows:

$$\left.\begin{aligned} \psi(x,y) &= \psi_0(x,y) + \varepsilon\psi_1(x,y) + O\left(\varepsilon^2\right), \\ \phi(x,y) &= \phi_0(x,y) + \varepsilon\phi_1(x,y) + O\left(\varepsilon^2\right), \\ t^m &= 1 + \varepsilon t_1^m + O\left(\varepsilon^2\right), \\ r^m &= \varepsilon r_1^m + O\left(\varepsilon^2\right), \\ T^m &= \varepsilon T_1^m + O\left(\varepsilon^2\right), \\ R^m &= \varepsilon R_1^m + O\left(\varepsilon^2\right), \end{aligned}\right\} \tag{16}$$

where $\psi_0(x,y)$ and $\phi_0(x,y)$ are given by (12) and (13) respectively.

Now substituting relation (16) in equations (1)-(5), (7), (14), (15) and then comparing the first order terms of ε on both sides of the equations, we have:

$$\nabla^2\psi_1 = 0 \quad -h \le y \le 0, \tag{17}$$

$$\nabla^2\phi_1 = 0 \quad 0 \le y \le H, \tag{18}$$

$$K\psi_1 + \left(1 - \delta K + D\frac{\partial^4}{\partial x^4}\right)\psi_{1y} = 0 \quad \text{on } y = -h \tag{19}$$

$$\phi_{1y} = \psi_{1y} \quad \text{on } y = 0, \tag{20}$$

$$\rho\left(K\psi_1 + \psi_{1y}\right) = K\phi_1 + \phi_{1y} \quad \text{on } y = 0, \tag{21}$$

$$\phi_{1y} - G\phi_1 = q(x) \quad \text{on } y = H, \tag{22}$$

where

$$q(x) \equiv \mathrm{i}m\frac{\mathrm{d}}{\mathrm{d}x}\left[c(x)\mathrm{e}^{\mathrm{i}mx}\right] + G^2 c(x), \tag{23}$$

and the far-field behaviors are:

$$\psi_1(x,y) \to \begin{cases} r_1^m f(m,y)\mathrm{e}^{-\mathrm{i}mx} + R_1^m f(M,y)\mathrm{e}^{-\mathrm{i}Mx} & \text{as } x \to -\infty, \\ t_1^m f(m,y)\mathrm{e}^{\mathrm{i}mx} + T_1^m f(M,y)\mathrm{e}^{\mathrm{i}Mx} & \text{as } x \to \infty, \end{cases} \tag{24}$$

and

$$\phi(x,y) \to \begin{cases} r_1^m \begin{bmatrix} \cosh m(H-y) \\ -\dfrac{G}{m}\sinh m(H-y) \end{bmatrix}\mathrm{e}^{-\mathrm{i}mx} + \\ \quad R_1^m \begin{bmatrix} \cosh M(H-y) \\ -\dfrac{G}{M}\sinh M(H-y) \end{bmatrix}\mathrm{e}^{-\mathrm{i}Mx} \quad \text{as } x \to -\infty, \\ t_1^m \begin{bmatrix} \cosh m(H-y) \\ -\dfrac{G}{m}\sinh m(H-y) \end{bmatrix}\mathrm{e}^{\mathrm{i}mx} + \\ \quad T_1^m \begin{bmatrix} \cosh M(H-y) \\ -\dfrac{G}{M}\sinh M(H-y) \end{bmatrix}\mathrm{e}^{\mathrm{i}Mx} \quad \text{as } x \to \infty, \end{cases} \tag{25}$$

3.2 Fourier transform technique

The solution of the above coupled BVP described by equations (17)−(22) for the potentials $\psi_1(x,y)$ and $\phi_1(x,y)$, is obtained by using the Fourier transform technique. Now to solve the coupled BVP, we decouple the BVP by replacing the condition (20) with:

$$\psi_{1y} = p(x) \quad \text{on} \quad y=0 \tag{26}$$

and

$$\phi_{1y} = p(x) \quad \text{on} \quad y=0 \tag{27}$$

where $p(x)$ is an unknown function.

Then the above BVP involving the relations (17)–(22) can be decomposed into two independent BVPs for ψ_1 and ϕ_1 as follows:

BVP-I, corresponding to ψ_1, is

$$\nabla^2\psi_1 = 0 \qquad -h \le y \le 0, \tag{28}$$

$$K\psi_1 + \left(1-\delta K + D\frac{\partial^4}{\partial x^4}\right)\psi_{1y} = 0 \quad \text{on } y=-h \tag{29}$$

$$\psi_{1y} = p(x) \qquad \text{on } y=0 \tag{30}$$

BVP-II, corresponding to ϕ_1, is

$$\nabla^2\phi_1 = 0 \qquad 0 \le y \le H \tag{31}$$

$$\phi_{1y} = p(x) \qquad \text{on} \quad y=0 \tag{32}$$

$$\phi_{1y} - G\phi_1 = q(x) \qquad \text{on} \quad y=H \tag{33}$$

Now using relations (30) and (32), relation (21) can be written as:

$$K(\phi_1 - \rho\psi_1) = (\rho-1)p(x) \qquad \text{on} \qquad y=0 \tag{34}$$

To solve the BPV-I and BVP-II, we assume that m and M have small positive imaginary parts so that ψ_1 and ϕ_1 decrease exponentially as $|x| \to \infty$. This ensures the existence of Fourier transforms $\hat{\psi}_1(k,y)$ and $\hat{\phi}_1(k,y)$ of $\psi_1(x,y)$ and $\phi_1(x,y)$ respectively, and are defined as:

$$\hat{\psi}_1(k,y) = \int_{-\infty}^{\infty}\psi_1(x,y)\mathrm{e}^{-\mathrm{i}kx}\mathrm{d}x, \tag{35}$$

with inverse

$$\psi_1(x,y) = \frac{1}{2\pi}\int_{-\infty}^{\infty}\hat{\psi}_1(k,y)\mathrm{e}^{\mathrm{i}kx}\mathrm{d}k \tag{36}$$

and

$$\hat{\phi}_1(k,y) = \int_{-\infty}^{\infty}\phi_1(x,y)\mathrm{e}^{-\mathrm{i}kx}\mathrm{d}x, \tag{37}$$

with inverse

$$\phi_1(x,y) = \frac{1}{2\pi}\int_{-\infty}^{\infty}\hat{\phi}_1(k,y)\mathrm{e}^{ikx}\mathrm{d}k. \tag{38}$$

Using Fourier transform in relations (28)-(30) we have:

$$\hat{\psi}_{1yy} - k^2\hat{\psi}_1 = 0 \qquad -h \le y \le 0, \tag{39}$$

$$K\hat{\psi}_1 + \left(1-\delta K + Dk^4\right)\hat{\psi}_{1y} = 0 \quad \text{on} \quad y=-h, \tag{40}$$

$$\hat{\psi}_{1y} = \overline{p}(k) \quad \text{on} \quad y=0, \tag{41}$$

where $\overline{p}(k)$ is the Fourier transform of $p(x)$.

Similarly, using Fourier transform in the relations (31)–(33) we get:

$$\hat{\phi}_{1yy} - k^2\hat{\phi}_1 = 0 \qquad 0 \le y \le H \tag{42}$$

$$\hat{\phi}_{1y} = \overline{p}(k) \qquad \text{on} \quad y=0 \tag{43}$$

$$\hat{\phi}_{1y} - G\hat{\phi}_1 = \overline{q}(k) \qquad \text{on} \quad y=H \tag{44}$$

where $\overline{q}(k)$ is the Fourier transform of $q(x)$.

Now the solutions of the above BVPs can be obtained in the term of $\overline{p}(k)$. Using the relation (34), the final solution for $\hat{\psi}_1(k,y)$ and $\hat{\phi}_1(k,y)$ are obtained as:

$$\hat{\psi}_1(k,y) = \frac{K\,\overline{q}(k)\left[K\sinh k(h+y) - \begin{pmatrix} Dk^4 \\ +1 \\ -\delta K \end{pmatrix} k\cosh k(h+y)\right]}{k\sinh kh\sinh kH\Delta(k)} \tag{45}$$

and

$$\hat{\phi}_1(k,y) = \frac{\overline{q}(k)}{(k\sinh kH - G\cosh kH)} \times \left[\cosh ky - \frac{K\begin{pmatrix} K\coth kh \\ -k\left(Dk^4+1-\delta K\right)\end{pmatrix}\begin{pmatrix} k\cosh k(H-y) \\ -G\sinh k(H-y)\end{pmatrix}}{k\sinh kH\Delta(k)}\right] \tag{46}$$

Using inverse Fourier transform we get $\psi_1(x,y)$ and $\phi_1(x,y)$ as follows:

$$\psi_1(x,y) = \frac{K}{2\pi}\int_0^{\infty}\frac{\left[K\sinh k(h+y) - \begin{pmatrix} Dk^4+1 \\ -\delta K\end{pmatrix} k\cosh k(h+y)\right]}{k\sinh kh\sinh kH\Delta(k)} \times\left[\overline{q}(k)\mathrm{e}^{ikx} + \overline{q}(-k)\mathrm{e}^{-ikx}\right]\mathrm{d}k \tag{47}$$

and

$$\phi_1(x,y) = \frac{1}{2\pi}\int_0^{\infty}\frac{1}{(k\sinh kH - G\cosh kH)} \times \left[\cosh ky - \frac{K\left(K\coth kh - k\begin{pmatrix} Dk^4 \\ +1 \\ -\delta K\end{pmatrix}\right)\begin{pmatrix} k\cosh k(H-y) \\ -G\sinh k(H-y)\end{pmatrix}}{k\sinh kH\Delta(k)}\right] \times \left[\overline{q}(k)\mathrm{e}^{ikx} + \overline{q}(-k)\mathrm{e}^{-ikx}\right]\mathrm{d}k, \tag{48}$$

where the path in each integral is intended below the poles at $k = m$, M.

Due to a normal incident wave of mode m, the first-order reflection and transmission coefficients can be obtained by letting $x \to \pm\infty$ in relation (47) or (48) and then comparing with relation (24) or (25).

Now, to obtain the first order transmission coefficients, we let $x \to \infty$ in either relation (47) or (48). As $x \to \infty$, then $\psi_1(x,y)$ or $\phi_1(x,y)$ can be obtained by rotating the path of the integral involving term e^{ikx} into a contour in the first quadrant by an angle β ($0<\beta<\pi/2$) and the contour in the integrals involving $\mathrm{e}^{-\mathrm{i}kx}$ in the fourth quadrant by the same angle so that the integral involving the term $\mathrm{e}^{-\mathrm{i}kx}$ does not contribute anything as $x\to\infty$. Then comparing the resultant integral value with the equations (24) or (25), we have:

$$t_1^m=\frac{\mathrm{i}K\left[\left(Dm^4+1-\delta K\right)m\sinh mh-K\cosh mh\right]}{\sinh mh\sinh mH\left(m\sinh mH-G\cosh mH\right)\Delta'(m)}\,\overline{q}(m) \tag{49}$$

and

$$T_1^m=\frac{\mathrm{i}K\left[\left(DM^4+1-\delta K\right)M\sinh Mh-K\cosh Mh\right]}{\sinh Mh\sinh MH\left(M\sinh MH-G\cosh MH\right)\Delta'(M)}\times\overline{q}(M), \tag{50}$$

where $\Delta'(k)$ is the derivative with respects to k.

Now using the value of $\overline{q}(m)$ and $\overline{q}(M)$ as given by:

$$\overline{q}(m)=\left(G^2-m^2\right)\int_{-\infty}^{\infty}c(x)\,\mathrm{d}x \tag{51}$$

and

$$\overline{q}(M)=\left(G^2-mM\right)\int_{-\infty}^{\infty}c(x)\,\mathrm{e}^{-\mathrm{i}(M-m)x}\mathrm{d}x, \tag{52}$$

we obtained the results for t_1^m and T_1^m as follows:

$$t_1^m=\frac{\mathrm{i}K\left[\left(Dm^4+1-\delta K\right)m\sinh mh-K\cosh mh\right]\times\left(G^2-m^2\right)}{\sinh mh\sinh mH\left(m\sinh mH-G\cosh mH\right)\Delta'(m)}\times\int_{-\infty}^{\infty}c(x)\,\mathrm{d}x \tag{53}$$

and

$$T_1^m=\frac{\mathrm{i}K\left[\left(DM^4+1-\delta K\right)M\sinh Mh-K\cosh Mh\right]\times\left(G^2-mM\right)}{\sinh Mh\sinh MH\left(M\sinh MH-G\cosh MH\right)\Delta'(M)}\times\int_{-\infty}^{\infty}c(x)\,\mathrm{e}^{-\mathrm{i}(M-m)x}\mathrm{d}x. \tag{54}$$

Similarly, to find the first order reflection coefficients, we let $x\to-\infty$ in either relation (47) or (48). As $x\to-\infty$, the behavior of $\psi_1(x,y)$ or $\phi_1(x,y)$ can be obtained by rotating the path of the integral involving term e^{-ikx}, into a contour in the first quadrant, so that we must include the residue term at $k=m$, M and the path of the integrals involving e^{ikx} is rotated into a contour in the fourth quadrant so that the integral involving the term e^{ikx} does not contribute as $x\to-\infty$. Then comparing the resultant integral value with equation (24) or (25), we obtain:

$$r_1^m=\frac{\mathrm{i}K\left[K\cosh mh-\left(Dm^4+1-\delta K\right)m\sinh mh\right]\times\left(G^2-m^2\right)}{\sinh mh\sinh mH\left(m\sinh mH-G\cosh mH\right)\Delta'(m)}\times\int_{-\infty}^{\infty}c(x)\,\mathrm{e}^{2\mathrm{i}mx}\mathrm{d}x \tag{55}$$

And

$$R_1^m=\frac{\mathrm{i}K\left[K\cosh Mh-\left(DM^4+1-\delta K\right)M\sinh Mh\right]\times\left(G^2-mM\right)}{\sinh Mh\sinh MH\left(M\sinh MH-G\cosh MH\right)\Delta'(M)}\times\int_{-\infty}^{\infty}c(x)\,\mathrm{e}^{\mathrm{i}(M+m)x}\mathrm{d}x. \tag{56}$$

When we consider a train of progressive waves of mode M to be at normal incident on the bottom topography, the same mathematical procedure, described above for the case of mode m, is followed to obtain the first-order reflection and transmission coefficients t_1^M, T_1^M, r_1^M and R_1^M. The final expressions are as follows:

$$t_1^M=\frac{\mathrm{i}K\left[\left(Dm^4+1-\delta K\right)m\sinh mh-K\cosh mh\right]\times\left(G^2-mM\right)}{\sinh mh\sinh mH\left(m\sinh mH-G\cosh mH\right)\Delta'(m)}\times\int_{-\infty}^{\infty}c(x)\,\mathrm{e}^{\mathrm{i}(M-m)x}\mathrm{d}x, \tag{57}$$

$$T_1^M=\frac{\mathrm{i}K\left[\left(DM^4+1-\delta K\right)M\sinh Mh-K\cosh Mh\right]\times\left(G^2-M^2\right)}{\sinh Mh\sinh MH\left(M\sinh MH-G\cosh MH\right)\Delta'(M)}\times\int_{-\infty}^{\infty}c(x)\,\mathrm{d}x, \tag{58}$$

$$r_1^M=\frac{\mathrm{i}K\left[K\cosh mh-\left(Dm^4+1-\delta K\right)m\sinh mh\right]\times\left(G^2-mM\right)}{\sinh mh\sinh mH\left(m\sinh mH-G\cosh mH\right)\Delta'(m)}\times\int_{-\infty}^{\infty}c(x)\,\mathrm{e}^{i(M+m)x}\mathrm{d}x, \tag{59}$$

and

$$R_1^M=\frac{\mathrm{i}K\left[K\cosh Mh-\left(DM^4+1-\delta K\right)M\sinh Mh\right]\times\left(G^2-M^2\right)}{\sinh Mh\sinh MH\left(M\sinh MH-G\cosh MH\right)\Delta'(M)}\times\int_{-\infty}^{\infty}c(x)\,e^{2iMx}\mathrm{d}x. \tag{60}$$

The above integral forms can be evaluated once the bottom profile $c(x)$ is known. In the next section, we consider a special form for the shape function $c(x)$.

4 Bottom profile

Davies (1982) found that an undulating bed has the ability to reflect incident wave energy which has an important implication for the application of coastal protection, and in the case of possible ripple growth if the bed is erodible. Here we consider a special form for the shape function $c(x)$ in the form of a patch of sinusoidal bottom ripples, which is considered as the bottom undulation. The following bottom undulation closely resembles some naturally occurring obstacles formed at the bottom due to sedimentation and ripple growth of sands:

$$c(x)=\begin{cases} a\sin\gamma x & \text{for } \dfrac{-n\pi}{\gamma}\le x\le\dfrac{n\pi}{\gamma},\\ 0 & \text{otherwise,}\end{cases} \tag{61}$$

where n is a positive integer. This represents a patch of sinusoidal ripples with amplitude a on an otherwise flat bottom, the patch consisting of n ripples having the same wave number γ. By substituting $c(x)$ given by (61), in relations (53)−(60), the first-order reflection and transmission coefficients can be obtained due to normal incident waves of both the modes m and M. Since $c(x)$ is an odd function, t_1^m, T_1^M vanish and the other coefficients are as follows:

$$r_1^m=(-1)^n\times\frac{K\left[K\cosh mh-\left(Dm^4+1-\delta K\right)m\sinh mh\right]\times\left(G^2-m^2\right)}{\sinh mh\sinh mH\left(m\sinh mH-G\cosh mH\right)\Delta'(m)}\times\frac{2a\gamma\sin\dfrac{2nm\pi}{\gamma}}{\gamma^2-4m^2}, \tag{62}$$

$$R_1^m=(-1)^n\times\frac{K\left[K\cosh Mh-\left(DM^4+1-\delta K\right)M\sinh Mh\right]\times\left(G^2-mM\right)}{\sinh Mh\sinh MH\left(M\sinh MH-G\cosh MH\right)\Delta'(M)}\times\frac{2a\gamma\sin\dfrac{n(M+m)\pi}{\gamma}}{\gamma^2-(M+m)^2}, \tag{63}$$

$$T_1^m=(-1)^{n+1}\times\frac{K\left[\left(DM^4+1-\delta K\right)M\sinh Mh-K\cosh Mh\right]\times\left(G^2-mM\right)}{\sinh Mh\sinh MH\left(M\sinh MH-G\cosh MH\right)\Delta'(M)}\times\frac{2a\gamma\sin\dfrac{n(M-m)\pi}{\gamma}}{\gamma^2-(M-m)^2}, \tag{64}$$

$$t_1^M=(-1)^{n+1}\times\frac{K\left[\left(Dm^4+1-\delta K\right)m\sinh mh-K\cosh mh\right]\times\left(G^2-mM\right)}{\sinh mh\sinh mH\left(m\sinh mH-G\cosh mH\right)\Delta'(m)}\times\frac{2a\gamma\sin\dfrac{n(M-m)\pi}{\gamma}}{\gamma^2-(M-m)^2}, \tag{65}$$

$$r_1^M=(-1)^n\times\frac{K\left[K\cosh mh-\left(Dm^4+1-\delta K\right)m\sinh mh\right]\times\left(G^2-mM\right)}{\sinh mh\sinh mH\left(m\sinh mH-G\cosh mH\right)\Delta'(m)}\times\frac{2a\gamma\sin\dfrac{n(M+m)\pi}{\gamma}}{\gamma^2-(M+m)^2} \tag{66}$$

and

$$R_1^M=(-1)^n\times\frac{K\left[K\cosh Mh-\left(DM^4+1-\delta K\right)M\sinh Mh\right]\times\left(G^2-M^2\right)}{\sinh Mh\sinh MH\left(M\sinh MH-G\cosh MH\right)\Delta'(M)}\times\frac{2a\gamma\sin\dfrac{2nM\pi}{\gamma}}{\gamma^2-4M^2}. \tag{67}$$

Relations (62)−(67) illustrate that for a given number of n ripples, the first order reflection and transmission coefficients due to incident waves of both modes are oscillatory in nature. Furthermore, at the critical conditions $\gamma=2m$ or $\gamma=M+m$ or $\gamma=M-m$ or $\gamma=2M$, the theory predicts a resonant interaction, namely the Bragg resonance (see Mei (1985), Alam *et al*. (2009) and others), between the bed and the surface or internal-mode wave. Hence, we find from the relations (62)-(67) that:

$$r_1^m=(-1)^n\times\frac{K\left[K\cosh mh-\left(Dm^4+1-\delta K\right)m\sinh mh\right]\times\left(G^2-m^2\right)}{\sinh mh\sinh mH\left(m\sinh mH-G\cosh mH\right)\Delta'(m)}\times\frac{an\pi}{2m}, \tag{68}$$

$$R_1^m=(-1)^n\times\frac{K\left[K\cosh Mh-\left(DM^4+1-\delta K\right)M\sinh Mh\right]\times\left(G^2-mM\right)}{\sinh Mh\sinh MH\left(M\sinh MH-G\cosh MH\right)\Delta'(M)}\times\frac{an\pi}{(M+m)}, \tag{69}$$

$$T_1^m=(-1)^{n+1}\times\frac{K\left[\left(DM^4+1-\delta K\right)M\sinh Mh-K\cosh Mh\right]\times\left(G^2-mM\right)}{\sinh Mh\sinh MH\left(M\sinh MH-G\cosh MH\right)\Delta'(M)}\times\frac{an\pi}{(M-m)}, \tag{70}$$

$$t_1^M=(-1)^{n+1}\times\frac{K\left[\left(Dm^4+1-\delta K\right)m\sinh mh-K\cosh mh\right]\times\left(G^2-mM\right)}{\sinh mh\sinh mH\left(m\sinh mH-G\cosh mH\right)\Delta'(m)}\times\frac{an\pi}{(M-m)}, \tag{71}$$

$$r_1^M=(-1)^n\times\frac{K\left[K\cosh mh-\left(Dm^4+1-\delta K\right)m\sinh mh\right]\times\left(G^2-mM\right)}{\sinh mh\sinh mH\left(m\sinh mH-G\cosh mH\right)\Delta'(m)}\times\frac{an\pi}{(M+m)}, \tag{72}$$

and

$$R_1^M=(-1)^n\times\frac{K\left[K\cosh Mh-\left(DM^4+1-\delta K\right)M\sinh Mh\right]\times\left(G^2-M^2\right)}{\sinh Mh\sinh MH\left(M\sinh MH-G\cosh MH\right)\Delta'(M)}\times\frac{an\pi}{2M}. \tag{73}$$

In this case the first order reflection and transmission coefficients become a constant multiple of n, the number of ripples in the patch. Although the theory breaks down when n becomes large and the solution is singular ($\gamma = 2m$ or $\gamma = M + m$ or $\gamma = M - m$ or $\gamma = 2M$), a large amount of reflection of the incident wave energy by the bed forms is predicted in the neighborhood of the singularity.

5 Numerical results and discussion

The first-order reflection and transmission coefficients given in relations (62)−(67) are computed numerically and are shown in for the different values of the different dimensionless parameters.

In Figs. 2−10, the reflection and transmission coefficients are plotted when an incident wave of wave number m is at normal incident on the undulation of the porous bottom.

$|r_1^m|$, $|R_1^m|$ and $|T_1^m|$ are plotted respectively in Figs. 2, 3, 4 against wave number Kh by considering the parameters $D/h^4 = 1$, $\delta/h = 0.01$, depth ratio $H/h = 2$, density ratio $\rho = 0.5$, the amplitude of the sinusoidal ripple $a/h = 1$, number of ripples $n = 3$ and wave number of ripples $\gamma h = 1$ for three different porous effect parameters $Gh = 0$, 0.01 and 0.02. From these figures, it is clear that $|r_1^m|$, $|R_1^m|$ and $|T_1^m|$ are oscillating in nature as a function of wave number Kh, which validates the theoretical observation obtained in section 4. The peak values of $|r_1^m|$, $|R_1^m|$ and $|T_1^m|$ are obtained respectively when $\gamma h = 2mh$ (the wave number of the undulating bottom becomes approximately twice the surface wave number), $\gamma h = (M + m)h$, $\gamma h = (M-m)h$. For these three different values of Gh, the peak value of $|r_1^m|$ is respectively given by 0.04115, 0.04048, 0.03981 (in Fig. 2); the peak value of $|R_1^m|$ is respectively given by 0.01108, 0.01236, 0.0138 (in Fig. 3) and the peak value of $|T_1^m|$ is given by 0.00475, 0.00478, 0.00484 (in Fig. 4) for certain values of Kh. From these numerical data, it is observed that at Bragg resonance the peak value of $|r_1^m|$ decreases as the value of the porous effect parameter increases whilst the peak value of $|R_1^m|$, $|T_1^m|$ increases as the porosity increases.

$|r_1^m|$, $|R_1^m|$ and $|T_1^m|$ are plotted for three different values of ice-cover parameter $D/h^4 = 1$, 3, 5 with $\rho = 0.5$, $n = 3$, $H/h = 2$, $\gamma h = 1$, $\delta/h = 0.01$ and $Gh = 0.01$ in Figs. 5, 6 and 7 respectively. From Figs. 5 and 6, we observe that the peak value of $|r_1^m|$ decreases while the peak value of $|R_1^m|$ increases as D/h^4 increases. But in Fig. 7, it is observed that there is an insignificant change in the transmission coefficient $|T_1^m|$ with the change in ice-cover parameter D/h^4. This is mainly due to the fact that the ice-cover is somewhat above the interface.

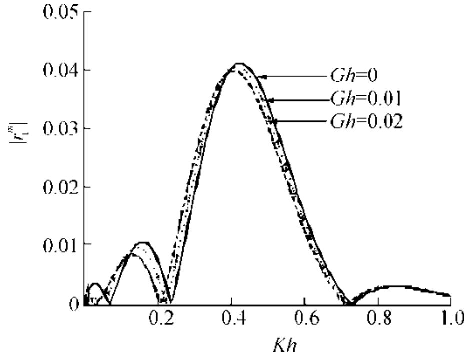

Fig. 2 Reflection coefficient at mode *m* due to an incident wave of mode *m* for $D/h^4 = 1$, $H/h = 2$, $\rho = 0.5$, $\gamma h = 1$, $\delta/h = 0.01$, $n = 3$.

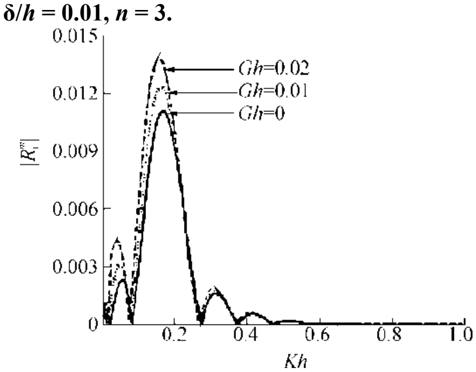

Fig. 3 Reflection coefficient at mode *M* due to an incident wave of mode *m* for $D/h^4 = 1$, $H/h = 2$, $\rho = 0.5$, $\gamma h = 1$, $\delta/h = 0.01$, $n = 3$.

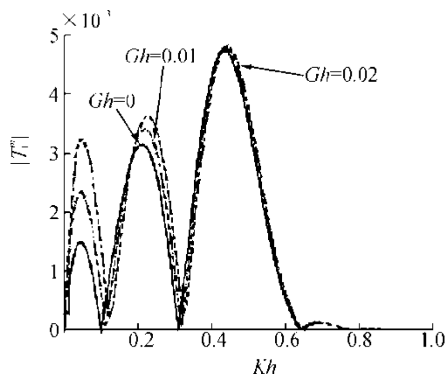

Fig. 4 Transmission coefficient at mode *M* due to an incident wave of mode *m* for $D/h^4 = 1$, $H/h = 2$, $\rho = 0.5$, $\gamma h = 1$, $\delta/h = 0.01$, $n = 3$.

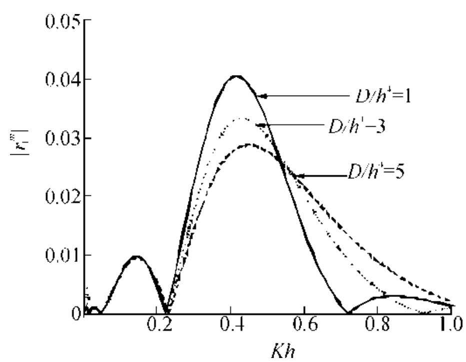

Fig. 5 Reflection coefficient at mode *m* due to an incident wave of mode *m* for $\rho = 0.5$, $n = 3$, $H/h = 2$, $\gamma h = 1$, $\delta/h = 0.01$, $Gh = 0.01$.

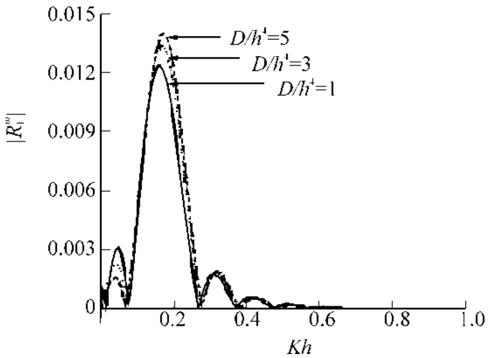

Fig. 6 Reflection coefficient at mode *M* due to an incident wave of mode *m* for ρ = 0.5, *n* = 3, *H*/*h* = 2, γ*h* = 1, δ/*h* = 0.01, *Gh* = 0.01.

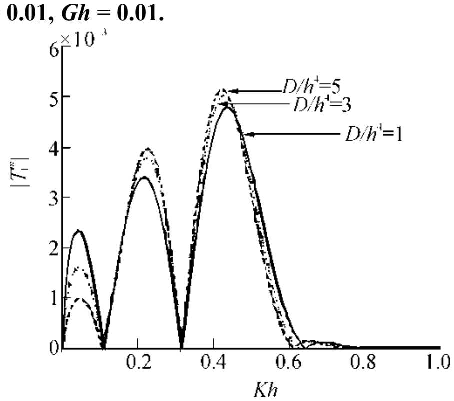

Fig. 7 Transmission coefficient at mode *M* due to an incident wave of mode *m* for ρ = 0.5, *n* = 3, *H*/*h* = 2, γ*h* = 1, δ/*h* = 0.01, *Gh* = 0.01.

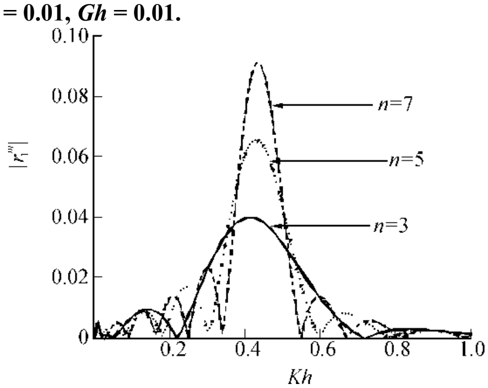

Fig. 8 Reflection coefficient at mode *m* due to an incident wave of mode *m* for ρ = 0.5, D/h^4 = 1, *H*/*h* = 2, γ*h* = 1, δ/*h* = 0.01, *Gh* = 0.01.

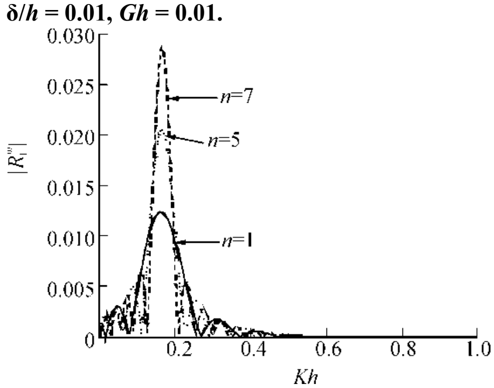

Fig. 9 Reflection coefficient at mode *M* due to an incident wave of mode *m* for ρ = 0.5, D/h^4 = 1, *H*/*h* = 2, γ*h* = 1, δ/*h* = 0.01, *Gh* = 0.01.

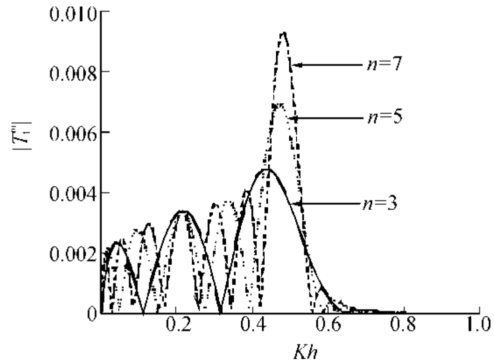

Fig. 10 Transmission coefficient at mode *M* due to an incident wave of mode *m* for ρ = 0.5, D/h^4 = 1, *H*/*h* = 2, γ*h* = 1, δ/*h* = 0.01, *Gh* = 0.01.

$|r_1^m|$, $|R_1^m|$ and $|T_1^m|$ are plotted respectively in Figs. 8, 9, 10 for three different values of number of ripples (*n* = 3, 5, 7) with D/h^4 = 1, ρ = 0.5, *H*/*h* = 2, γh = 1, δ/h = 0.01 and *Gh* = 0.01. In each of these figures, the peak value of the coefficients increases as the number of ripples increases. Thus, if the number of ripples increases indefinitely, the first-order coefficients become unbounded for certain values of *Kh* and this is known as Bragg resonance, due to which the perturbation analysis fails as described by Mei (1985).

The first-order reflection and transmission coefficients are plotted against the wave number *Kh* for the incident wave of mode *M* as shown in figures 11-19.

$|r_1^M|$, $|t_1^M|$ and $|R_1^M|$ are plotted against wave number *Kh* in Figs. 11, 12, 13 respectively for three different values of the number of ripples (*n* = 3, 5, 7) with D/h^4 = 1, δ/h = 0.01, *H*/*h* = 2, ρ = 0.5, *a*/*h* = 1, γh = 1 and *Gh* = 0.01. In each of these

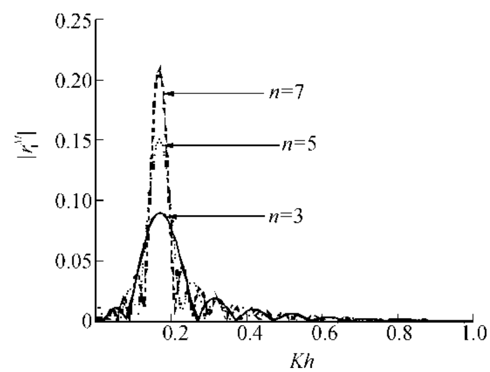

Fig. 11 Reflection coefficient at mode *m* due to an incident wave of mode *M* for ρ = 0.5, D/h^4 = 1, *H*/*h* = 2, γ*h* = 1, δ/*h* = 0.01, *Gh* = 0.01.

Figs. 11−13, it is observed that the peak value of the coefficients increases as the number of ripples increases. Here also, if the number of ripples increases indefinitely, the first-order coefficients become unbounded for a certain value of *Kh* as observed in Figs. 8−10 for an incident wave of mode *m*. The same remark made earlier about Bragg resonance also applies here.

$|r_1^M|$, $|t_1^M|$ and $|R_1^M|$ are plotted in Figs. 14, 15, and 16 respectively for three different values of the ice-cover parameter ($D/h^4 = 1, 3, 5$) with $\rho = 0.5$, $H/h = 2$, $\gamma h = 1$, $\delta/h = 0.01$, $a/h = 1$, $n = 3$ and $Gh = 0.01$. From these figures, it is clear that the values of the $|r_1^M|$ and $|R_1^M|$ are almost the same with the increase of the ice parameter D/h^4 due to the fact that the train of waves of mode M propagate along the interface while from Fig. 16, we observe that the peak value of $|t_1^M|$ decreases with the increase of D/h^4.

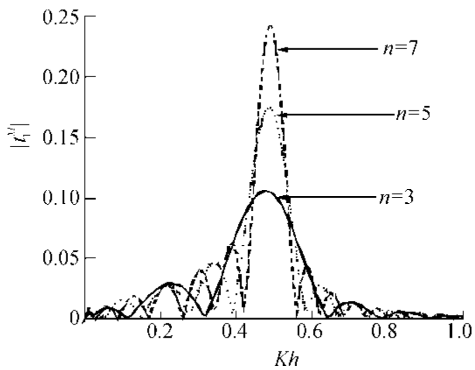

Fig. 12 Transmission coefficient at mode *m* due to an incident wave of mode *M* for $\rho = 0.5$, $D/h^4 = 1$, $H/h = 2$, $\gamma h = 1$, $\delta/h = 0.01$, $Gh = 0.01$.

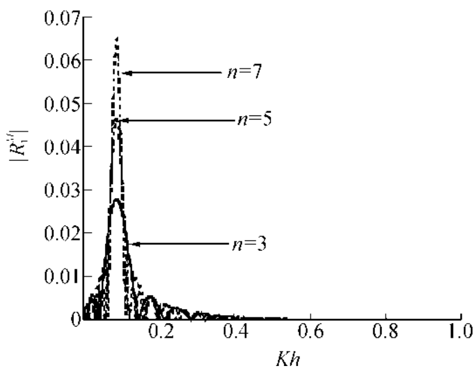

Fig. 13 Reflection coefficient at mode *M* due to an incident wave of mode *M* for $\rho = 0.5$, $D/h^4 = 1$, $H/h = 2$, $\gamma h = 1$, $\delta/h = 0.01$, $Gh = 0.01$.

$\left|r_1^M\right|$, $\left|t_1^M\right|$ and $\left|R_1^M\right|$ are plotted respectively in Figs. 17, 18, and 19 for different values of the porous effect parameter (Gh = 0, 0.01, 0.02) with $D/h^4 = 1$, $\delta/h = 0.01$, $H/h = 2$, $\rho = 0.5$, $a/h = 1$, $\gamma h = 1$ and $n = 3$. From these figures it is clear that the peak values of $\left|r_1^M\right|$ and $\left|t_1^M\right|$ decreases while the reflection coefficient $\left|R_1^M\right|$ increases as the porous effect parameters increase.

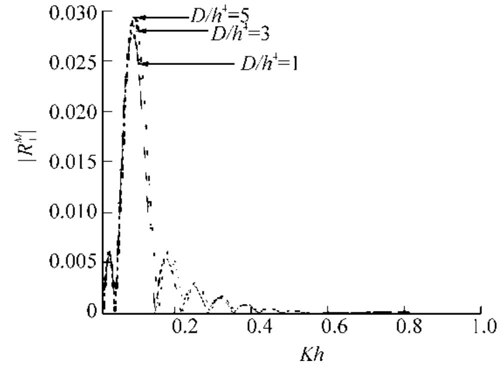

Fig. 14 Reflection coefficient at mode *M* due to an incident wave of mode *M* for $\rho = 0.5$, $n = 3$, $H/h = 2$, $\gamma h = 1$, $\delta/h = 0.01$, $Gh = 0.01$.

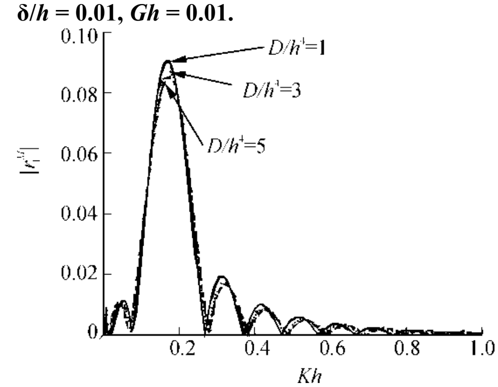

Fig. 15 Reflection coefficient at mode *m* due to an incident wave of mode *M* for $\rho = 0.5$, $n = 3$, $H/h = 2$, $\gamma h = 1$, $\delta/h = 0.01$, $Gh = 0.01$.

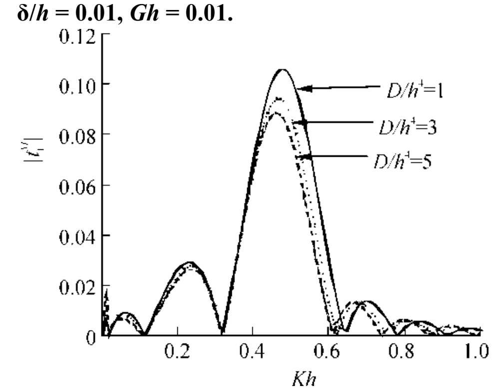

Fig. 16 Transmission coefficient at mode *m* due to an incident wave of mode *M* for $\rho = 0.5$, $n = 3$, $H/h = 2$, $\gamma h = 1$, $\delta/h = 0.01$, $Gh = 0.01$.

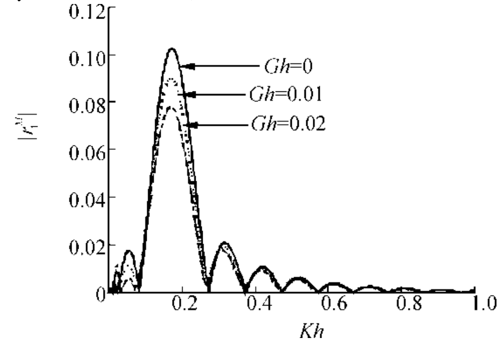

Fig. 17 Reflection coefficient at mode *m* due to an incident wave of mode *M* for $\rho = 0.5$, $D/h^4 = 1$, $H/h = 2$, $\gamma h = 1$, $\delta/h = 0.01$, $n = 3$.

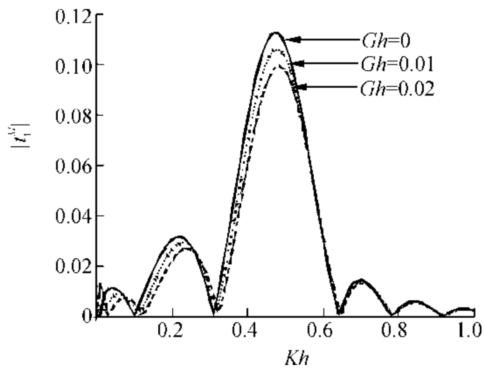

Fig. 18 Transmission coefficient at mode *m* due to an incident wave of mode *M* for ρ = 0.5, D/h^4 = 1, H/h = 2, γh = 1, δ/h = 0.01, *n* = 3.

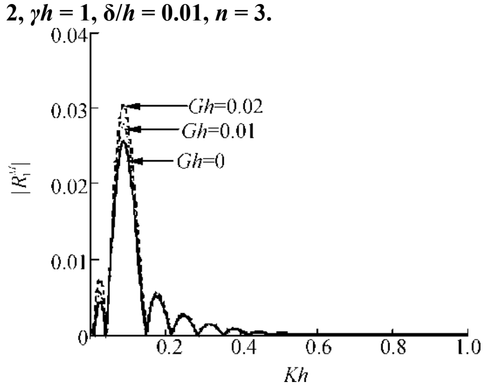

Fig. 19 Reflection coefficient at mode *M* due to an incident wave of mode *M* for ρ = 0.5, D/h^4 = 1, H/h = 2, γh = 1, δ/h = 0.01, *n* = 3.

6 Conclusion

The problem of water wave scattering by small undulation at the porous bottom of a two-layer ocean in which the upper layer is covered by a thin elastic uniform sheet of ice, is considered here for its solution. The BVPs which are derived from the physical problem are solved by using perturbation analysis in conjunction with the Fourier transform technique and the first order velocity potentials, reflection and transmission coefficients are obtained. The main advantage of this Fourier transform method is that we solve relatively easier ordinary differential equations to find the velocity potentials. Furthermore, the numerical results for the reflection and transmission coefficients are evaluated for a particular case of undulation, namely a patch of sinusoidal ripples. From the numerical results it is observed that, the reflection corresponding to the surface wave mode decreases while the reflection coefficient corresponding to the interface mode increases with the flexural rigidity of the ice-cover due to an incident wave of lower wave number (*m*). But the transmission coefficient corresponding to the interface mode remains unaffected by the flexural rigidity of the ice-cover.

When the incident wave is of higher wave number (*M*), the value of the reflection and transmission coefficients corresponding to the surface mode decreases while the value of the reflection coefficient corresponding to the interface mode increases as the flexural rigidity of the ice-cover increases. The reflection and transmission increases as the number of ripples of the porous ocean-bed increases due to the incident progressive wave of both modes. The reflection and transmission coefficients corresponding to the surface mode decrease while the reflection at the interface mode increases as the porosity increases. Especially, the concept of porosity may be useful for a class of scattering problems in the areas of coastal and marine engineering. The problems involving ice cover of variable thickness and the sea-bed consisting of arbitrary undulations will be the subject matter of our future investigations.

Acknowledgements

Srikumar Panda is grateful to the Council of Scientific and Industrial Research (CSIR), Government of India, for providing the Senior Research Fellowship to allow him to pursue his Ph.D. at the Indian Institute of Technology Ropar, India. S. C. Martha thanks the Indian Institute of Technology Ropar, India for their support through the ISIRD grant (Ref. No. 16-3/10/IITRPR/Acad/116) and for providing all the necessary facilities.

References

Alam MR, Liu Y, Yue DKP (2009). Bragg resonance of waves in a two-layer fluid propagating over bottom ripples Part I. Perturbation analysis. *Journal of Fluid Mechanics*, **624**, 191-224.

An Z, Ye Z (2004). Band gaps and localization of water waves over one-dimensional topographical bottoms. *Applied Physics Letters*, **84**(15), 2952-2954.

Bhatta DD, Debnath L (2006). Two layer transient water waves over a viscoelastic ocean bed. *Journal of Applied Mathematics and Computing*, **22**, 133-147.

Chakrabarti A (1989). A note on the porous-wavemaker problem. *Acta Mechanica*, **77**, 121-129.

Chakrabarti A (2000). On the solution of the problem of scattering of surface water waves by the edge of an ice-cover. *Proceedings of the Royal Society of London Series A*, **456**, 1087-1099.

Chamberlain PG, Porter D (2005). Wave scattering in a two-layer fluid of varying depth. *Journal of Fluid Mechanics*, **524**, 207-228.

Christodoulides P, Dias F (1995). Stability of capillary-gravity interfacial waves between two bounded fluids. *Physics of Fluids*, **7**(12), 3013-3027.

Chung H, Fox C (2002). Calculation of wave-ice interaction using the Wiener-Hopf technique. *New Zealand Journal of Mathematics*, **31**, 1-18.

Davies AG (1982). The reflection of wave energy by undulation on the seabed. *Dynamics of Atmospheres and Oceans*, **6**, 207-232.

Devillard P, Dunlop F, Souillard B (1988). Localization of gravity waves on a channel with a random bottom. *Journal of Fluid Mechanics,* **186**, 521-538.

Davies AG, Heathershaw AD (1984). Surface-wave propagation over sinusoidally varying topography. *Journal of Fluid Mechanics,* **144**, 419-443.

Fox C, Squire VA (1994). On the oblique reflection and transmission of ocean waves at shore fast sea ice. *Proceedings of the Royal Society of London Series A*, **347**, 185-218.

Gu Z, Wang H (1991). Gravity waves over porous bottoms. *Coastal Engineering*, **15**, 497-524.

Guazzelli E, Guyon E, Souillard B (1983). On the localization of shallow water waves by a random bottom. *Journal de Physique Lettres*, **44**, 837-841.

Jeng DS (2001). Wave dispersion equation in a porous seabed. *Coastal Engineering*, **28**, 1585-1599.

Lamb H (1932). *Hydrodynamics.* 6th ed, Cambridge University Press, Cambridge.

Linton CM, Cadby JR (2002). Scattering of oblique waves in a two-layer fluid. *Journal of Fluid Mechanics*, **461**, 343-364.

Linton CM, McIver M (1995). The interaction of waves with horizontal cylinders in a two-layer fluids. *Journal of Fluid Mechanics*, **304**, 213-229.

Maiti P, Mandal BN, Basu U (2009). Wave scattering by undulating bed topography in a two-layer ocean. *Journal of Marine Science and Application*, **8**, 183-195.

Martha SC, Bora SN (2007). Oblique surface wave propagation over a small undulation on the bottom of an ocean. *Geophysical & Astrophysical Fluid Dynamics*, **101**(2), 65-80.

Martha SC, Bora SN, Chakrabarti A (2007). Oblique water-wave scattering by small undulation on a porous sea-bed. *Applied Ocean Research*, **29**, 86-90.

Mase H, Takeba K (1994). Bragg scattering of gravity waves over porous ripple bed. *Proceedings of 24th Conference on Coastal Engineering*, Kobe, Japan: ASCE. **6**, 635-649.

Mei CC (1985). Resonant reflection of surface waves by periodic sandbars. *Journal of Fluid Mechanics*, **152**, 315-335.

Miles JW (1981). Oblique surface wave diffraction by a cylindrical obstacle. *Dynamics of Atmospheres and Oceans*, **6**, 121-123.

Mohapatra S, Bora SN (2009). Scattering of internal waves in a two-layer fluid flowing through a channel with small undulations. *Ocean Dynamics*, **59**, 615-625.

Mohapatra S, Bora SN (2012). Oblique water wave scattering by bottom undulation in a two-layer fluid flowing through a channel. *Journal of Marine Science and Application*, **11**, 276-285.

Olbers DJ (1981). A formal theory of internal wave scattering with applications to ocean fronts. *Journal of Physical Oceanography*, **11**, 1078-1099.

Silva R, Salles P, Palacio A (2002). Linear wave propagating over a rapidly varying finite porous bed. *Coastal Engineering*, **44**, 239-260.

Sveen JK, Guo Y, Davies PA, Grue J (2002). On the breaking of internal solitary waves at a ridge. *Journal of Fluid Mechanics*, **469**, 161-188.

Tkacheva LA (2001). Hydroelastic behavior of a floating plate in waves. *Journal of Applied Mechanics and Technical Physics*, **42**, 991-996.

Zhu S (2001). Water waves within a porous medium on an undulating bed. *Coastal Engineering*, **42**, 87-101.

Author biographies

Srikumar Panda received his M. Sc. in Mathematics and Computing from the Indian Institute of Technology, Guwahati, India in 2010. He is now studying as a Ph.D. student at the Indian Institute of Technology, Ropar, India under the CSIR Senior Research Fellowship. His main areas of interest are water wave scattering in a multilayered fluid, nonlinear fluid flow problems and Singular Integral Equations.

Subash Chandra Martha is an Assistant Professor at the Department of Mathematics, Indian Institute of Technology Ropar, India. He received his Ph.D. from the Indian Institute of Technology, Guwahati, India in 2007. He also worked as a NBHM post doctoral fellow at the Indian Institute of Science, Bangalore, India. His main areas of interest are Fluid dynamics, Mathematical modeling on water wave phenomena and Integral Equations.